



Shape transition and coalescence of Au islands on Ag (110) by molecular dynamics simulation

F. Eddiai¹ · M. Dardouri² · A. Hassani^{1,2} · A. Hasnaoui¹ · K. Sbiaai¹

Received: 16 April 2020 / Accepted: 14 March 2021 / Published online: 5 April 2021
© The Author(s), under exclusive licence to Springer-Verlag GmbH Germany, part of Springer Nature 2021

Abstract

We have used molecular dynamics simulations based on many body semi-empirical potentials described by the embedded atom method, to analyze and understand the diffusion and coalescence phenomena of Au-clusters during the heteroepitaxial growth on Ag (110) surface. Temperature ranging from 300 to 700 K were considered. In this study, we examined the heterogeneous system $Au_n/Ag(110)$, where n is the number of atoms in each cluster/island (with $n = 15, \dots, 35$). Our results show that the clusters diffuse on the Ag (110) surface via different diffusion processes, namely, the exchange mechanism and the simple jump, which generate a 2D to 3D transition. Formation and adsorption energies of clusters with different sizes have been computed using static simulations. The dynamic study of coalescence for two islands of system $Au_{15}; Au_{0-9}/Ag(110)$ at different temperatures makes it possible to deduce the detail of cluster shape and the influence of its temperature on the stability of the system and its growth during this evolution.

Keywords Island shape transition · Molecular dynamics simulation · Adatom diffusion · Coalescence

Introduction

Island growth is often one of stages of thin film epitaxy and therefore relevant to the manufacture of a wide variety of interfacial materials. The electrical and mechanical properties of these products strongly depend on the surface roughness, the composition, and the microstructure [1–5]. These electronic, magnetic, optical, and chemical properties of noble metal nanoparticles are strongly influenced by size [6–11]; therefore, it is essential to study and understand the mechanisms involved in the growth of clusters and the effect of their size on cluster properties. Due to the need to obtain smooth and uniform surfaces, the study of the phenomenon of coalescence and the growth of islands makes it possible to control and understand the surface roughness [12–15].

In literature, several experimental and theoretical studies have highlighted this investigation [16–21], and now the ability to predict and control the size of clusters is of considerable importance to technological applications [22, 23]. Indeed the mechanism of growth, in particular, the coalescence of nanoparticles is a key element to predict and control the cluster size [24, 25].

The study of diffusion of isolated adatoms on metallic surfaces is an important step in the understanding of many properties of technological interest, for example, in the fields of growth and catalysis of thin films [3, 26]. Ag films developed on Au(111) and W(110) epitaxial thin films were studied by angle resolved photoemission [27].

Several results of the diffusion behavior of Rh and Ir tetramers on the surface Ir(001), show that from the diffusion of small islands of Pd with 2 to 9 Pd atoms on the surface W(110) can form a one- or two-dimensional island. The stability of linear chains remains up to eight atoms [18, 28, 29].

The process of growing an island can be divided into three stages. The first step is a nucleation process [30, 31] during which the rate of large island formation becomes greater and depends mainly on thermal activation [32]. The second step is the growth of clusters that is made by the attachment of an adatom to an island in order to achieve large cluster formation [10, 33]. The third stage is devoted to the growth of islands by

✉ F. Eddiai
f.eddiai.fpk@gmail.com

✉ K. Sbiaai
ksbiaai@gmail.com

¹ Laboratory LS3M, Polydisciplinary Faculty, Sultan Moulay Slimane University of Beni Mellal, 25000 Khouribga, Morocco

² Laboratory LPMC, Chouaib Doukkali University, El Jadida, Morocco

the phenomenon of coalescence [34, 35]. During this growth phase, the two affected clusters are normally larger.

The growth of small islands of Au on silver has been studied theoretically and experimentally [35, 36]. These studies consisted mainly of investigating islands coalescence on thin layers and their evolution through several diffusion mechanisms [37, 38].

Since thin-film epitaxy occurs frequently outside equilibrium, kinetics, deposition, and surface-scattering dynamics play a key role in island morphology and we obtain a great variety in the resulting microstructures [39, 40].

The monitoring of these phenomena of growth at the experimental time scale is very difficult, so part of the reality is missing. To access the atomistic scale information of diffusion mechanisms involved in this growth, molecular dynamics (DM) simulation remains a powerful and useful tool for this challenge. This method has a long history and has evolved into an important and widely used theoretical tool. MD simulation enables researchers in chemistry, physics, and biology to model the detailed microscopic dynamic behavior of many different types of systems, including gases, liquids, solids, surfaces, and clusters.

The temperatures at which these processes occur and the shape and size of islands are extremely important factors in determining the coalescence of islands of atoms on the surface of substrate.

The aim of this work is to study the effect of size and temperature on the coalescence of islands for different forms through diffusion mechanisms and their energy barriers. In this study, the stability of these islands is investigated.

Model and computational details

The spatiotemporal evolution of atoms is determined by solving the classical equations of motion, which are integrated by the usual Euler algorithm. As is well known, metals cannot be correctly modeled by pairs potentials (as Lennard-Jones and Morse), but many body potentials are needed. Among these, we have chosen the embedded atom method (EAM) developed by Daw and Baskes [41] to describe the interactions in some metals. These potentials have been successfully applied in the calculation of the properties of nanoparticles and bulk materials. For the used mixing rules, we used the method developed by Zhou et al. [41] who combined monoatomic EAM potential to describe heterogeneous systems. These potentials have been successfully used for surface studies in AgCu alloys [27, 42, 43]. The EAM is based on the functional theory of local density, which states that the energy of a solid can be written as a unique function of electron density, which is assumed to be the local density at each atomic site. The local electron density at the level of an atom is approximated by the superposition of the atomic electron densities of the

surrounding atoms; the total energy given by the EAM can be expressed as follows:

$$E_{tot} = \sum_i F_i(\rho_i) + \frac{1}{2} \sum_i \sum_{j(\neq i)} \varphi_{ij}(r_{ij}) \quad \text{With } \rho_i = \sum_{i(j\neq i)} \rho_j^\alpha(r_{ji}) \quad (1)$$

ρ_i is the sum of the individual electron density ρ_j^α provided by the other atoms of the system, $F_i(\rho_i)$ is the energy required to embed atom i into the local electron charge density ρ_i , $\varphi_{ij}(r_{ij})$ is a pairwise electrostatic interaction between atom i and atom j separated by the distance r_{ji} .

In this work, we have focused on the diffusion of Au_n clusters and their coalescence on Ag(110) substrate. Diffusion of clusters with sizes from $n = 15$ to 35 is considered while coalescence involved Au_{15} clusters with $Au_n (n = 0, 2, \dots, 9)$ on the same surface. During the 2D to 3D transition, many mechanisms are observed; these processes contribute to the coalescence between islands. The Verlet algorithm is used to solve Newton's equations of motion, with a time step of 1 fs. The simulated substrate consists of a two-sided free (110) surfaces containing 10 layers having (20×20) atoms in each layer. Here, the x and y axes are located in the plane of the surface, while the z -axis is perpendicular to the surface (Fig. 1). 2D geometries are formed by placing several atoms close together on the top side of the (110) surface. Periodic boundary conditions were performed in the surface plane while the surface perpendicular to z direction is taken free. The substrate was divided into three regions: free region (top 3 layers to enable deposition); isothermal region (3 layers in the middle absorb the kinetic energy), and a fixed region (4 bottom layers to prevent drifting the substrate).

All simulations start by generating a substrate along the desired orientation followed by an energy minimization. Then a cluster is deposited on the surface of the sample by matching the hollow sites of the (110) surface. During the

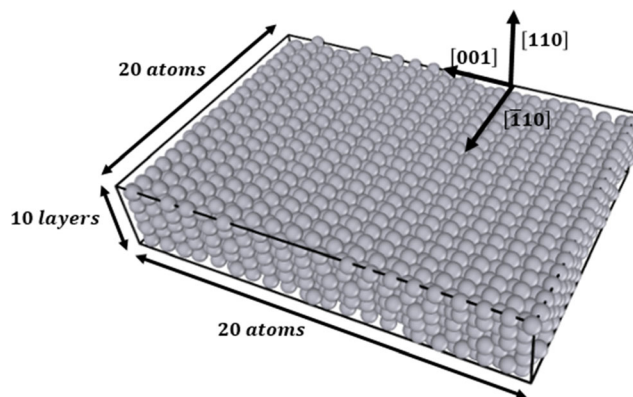


Fig. 1 Three-dimensional view of the substrate construction with three regions: free region (3 layers at the top); isothermal region (3 layers in the middle), and a fixed region (4 layers in the bottom)

static study, the geometry optimization is performed at 0 K by minimizing the energy using a conjugate gradient. For the dynamic study, we initially relaxed the substrate structure for 40 ps under NVT ensemble at the desired temperature before investigating the cluster diffusion.

In these static surveys, the activation energy is calculated using the drag method, which is the simplest and most commonly used method to find the transition state. In this method, the adatom is moved from its starting point to the nearest neighbor along the reaction path in small increments. At each step of the diffusion path, the total energy of the system is minimized.

Results and discussion

In the following, we will scroll through all the results obtained during the static and dynamic study of islands diffusion, as well as, the coalescence of two Au islands Au_n and $Au_m/Ag(110)$ for temperatures ranging between 300 K and 700 K. We will determine the formation and adsorption energies for the different clusters. Different parameters that characterize the dynamic evolution of these islands such as diffusion response time and 2D to 3D transition time will be studied as a function of the cluster size and temperature.

Static study

To describe the mechanisms of growth surface by coalescence islands, we need to take into account barrier energies for in-channel and cross-channel diffusion. In Fig. 2, we schematized the different possible diffusion mechanisms on the (110) surface.

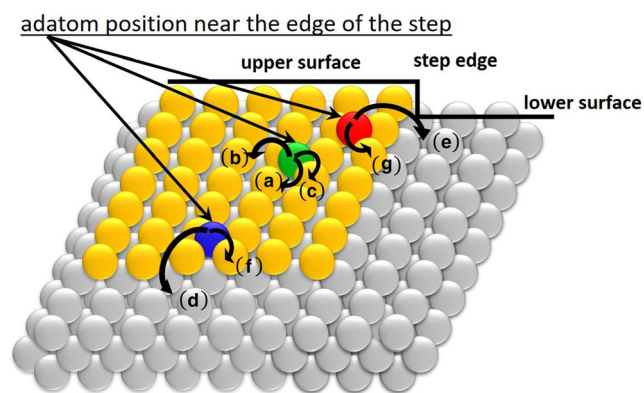


Fig. 2 Three-dimensional view of the geometric structure of the system illustrating the different possible adatom diffusion processes. On the terrace: (a) in-channel (IC) single jump, (b) cross-channel (CC) single jump, and (c) exchange (Ex) jump. Near the step: (d) in-channel direct jump, (e) cross-channel direct jump, and (f) and (g) Exchange jumps. In this representation, the green, blue, and red spheres represent the diffusing adatoms, the yellow spheres stand for atoms from the upper side of the step and gray color refer to atoms of the substrate

In Table 1, we summarized all energy values that will be needed in our study of heterogeneous systems. We should mention that Sbiaai et al. [32] have showed that there is no size effect on barrier energies for slab geometries beyond 6 layers.

The first statement that can be learned from Table 1 is the effect of anisotropic surface on the diffuse energy. It can be remarked that for the different diffusion processes in cross-channel is more expensive in terms of energy than that of in-channel diffusion. In homogeneous systems, Au/Au and Ag/Ag on (110) surface, the activation of adatom diffusing IC are 0.25 eV and 0.31 eV respectively, these values for CC are 0.62 eV and 0.78 eV, respectively. According to the energy activation for heterogeneous systems, we conclude that the CC diffusion (1.21 eV for Au/Ag and 1.25 eV for Ag/Au) are energetically very expensive than those of IC (0.30 eV for Au/Ag and 0.26 eV for Ag/Au). Concerning the hopping jump energy (Schwoebel barrier), we noticed that it is comparable for the different systems and is of the same order of the IC activation energy.

Firstly, an energy study was carried out based on the EAM method, detailing the process of formation energies and also adsorption energies for clusters of different sizes $Au_n/Ag(110)$ (with $15 \leq n \leq 35$) at 0 K. The adsorption energy E_{ad} is computed by the following formula:

$$E_{ad} = E_{tot}(0) - E_{tot}(n) \quad (2)$$

where $E_{tot}(0)$ is the energy of the slab without the adatom and $E_{tot}(n)$ is the energy of the slab with the cluster.

After adsorption of adatoms on the free surface, the clusters of different sizes are formed. Next, it is necessary to determine their stability by computing the binding energy for each cluster. From another side, the formation energy E_f is calculated via equation:

$$E_f = E_{tot}^* - E_{tot}(n) \quad (3)$$

where E_{tot}^* is the energy of the system containing the substrate with n isolated adatoms.

From the results shown in Table 2, we can see that the adsorption energy increases proportionally with the cluster size. We computed the per-atom adsorption (E_{ad}/n) and found that it varies slightly for small cluster and converges to 3.86 eV for large clusters. This is explained by the fact that adding an adatom to the cluster will generate the same additional number of bonds for large clusters while this is not the same for small clusters. For each size, it can be seen that the adsorption energy is higher than the formation one, which is explained by the attractive interaction of adatoms of the island with the substrate. These results represent a good agreement with other results in the systems $Zr_n/Zr(0001)$ and $Pt_n/Pt(111)$ [46, 47].

Table 1 In-channel (IC) and cross-channel (CC), diffusion barriers of different processes occurring for an adatom on a (110) surface

System (110)	E_a (eV)		E_{ex} (eV)	E_s (eV)		E_{sex} (eV)	
	IC	CC		IC	CC	IC	CC
Au/Au	0.25; (0.27 ^a , 0.28 ^{ab})	0.62	0.46 (0.42 ^c)	0.22	0.22	0.17	0.18
Ag/Ag	0.31; (0.31 ^b , 0.38 ^e)	0.78	0.31 (0.38 ^e)	0.18	0.19	0.17	0.19
Au/Ag	0.30; (0.25 ^d , 0.29 ^d)	1.21	0.35	0.20	0.20	0.19	0.21
Ag/Au	0.26, (0.27 ^e)	1.25	0.52	0.18	0.21	0.18	0.18

E_a activation energy, E_{ex} exchange energy, E_s , E_{sex} Ehrlich-Schwoebel energy at 0 K

^a From Ref. [44]

^b From Ref. [24]

^c From Ref. [42]

^d From Ref. [43]

^e From Ref. [45]

Dynamic study

In this section, we focused on the dynamic evolution of Au_n ($n = 15, \dots, 35$) islands on Ag(110) surface during a time of 10 ns at different temperatures ranging from 300 to 700 K. This study focused on the island forms shown in Table 2. The obtained results have shown that for low temperatures (≤ 500 K) the diffusion mechanism is not activated, while beyond this temperature, we have found that the islands evolve from 2D to 3D forms through several diffusion processes as we will show in the following. However, at high temperatures (> 650 K), we observed the disintegration of islands; it is the reason to limit this study to temperatures between 500 K and 650 K.

Figure 3 presents an example of these processes for a cluster Au_{15} at 550 K. We observe from this figure that an adatom is detached from the Au_{15} island by a simple jump at $t = 68$ ps (Fig. 3a), then it performs an exchange with an adatom of the substrate (Fig. 3b). During this evolution, we noticed that the structure underwent a transition from 2D to 3D after 61 ps leading finally to the formation of a heterogeneous dimer at $t = 183$ ps (Fig. 3c). This transition occurs in order to obtain a heterogeneous linear 3D trimer along the channel which remains stable. Similar results were obtained by field ion microscope (FIM) for the evolution of Rh_4 and Ir_4 on Ir(001) [18].

Figure 4 shows the dynamic evolution of Au_{21} island on Ag(110) at 650 K. This island began its diffusion by the detachment process and then the exchange with an adatom of the

substrate (Fig. 4a) in a short time (a few picoseconds). At this temperature, we notice a 2D to 3D transition via the formation of a homogeneous dimer at $t = 47$ ps (Fig. 4b), followed by the formation of two heterogeneous trimers (Fig. 4c) and finally the formation of a 3D structure consisting of 9 heterogeneous adatoms that remains stable during the evolution up to 10 ns.

Figure 5 presents the dynamic evolution of Au_{24} island on Ag(110) at 600 K. For this cluster, an adatom of the substrate triggers the 3D transition at $t = 74$ ps (Fig. 5b) by jumping on the cluster, then another adatom joins the first to form a heterogeneous dimer at $t = 210$ ps (Fig. 5c), finally, a third adatom rejoins this dimer to form a linear trimer along the channel (stable form) at $t = 469$ ps (Fig. 5d). These results are in good agreement with several theoretical and experimental studies that have been devoted to investigate the stability of island shape [25]. Indeed, Fu et al. [28] highlighted for Pd clusters on the W(110) surface that Pd cluster (< 8 adatoms) can form a stable 1D island strips or a 2D compact island.

Figure 6 shows the dynamic evolution of Au_{30} island on Ag(110) at 650 K. After 66 ps, this cluster starts diffusion by 3D transition involving 3 heterogeneous adatoms (Fig. 6b). Then, we observe the formation of a homogeneous linear 3D tetramer at $t = 184$ ps (Fig. 6c) triggered by thermal activation. We notice that this structure is a stable shape as already seen and suggested in ref. [32]. Finally, a substrate dimer jumped over to form the final 3D structure (Fig. 6d).

To analyze the stability of islands, we computed their lifetime as the elapsed time necessary for each temperature to dissociate the cluster (the length of time the island retains the initial shape). Figure 7 plots this lifetime for the various considered islands (when the response time lasts longer the island is stable). We see from this figure that for low temperatures (< 400 K), all clusters have a high resistivity to dissociation and can last for more than 10 ns. When temperature increases, we observe that the clusters lose their resistance showing temporal avalanches up at

Table 2 Formation and adsorption energies (eV) of islands of different sizes for the system $Au_n/Ag(110)$ ($n = 15$ à 35) at 0 K

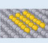

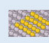



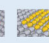
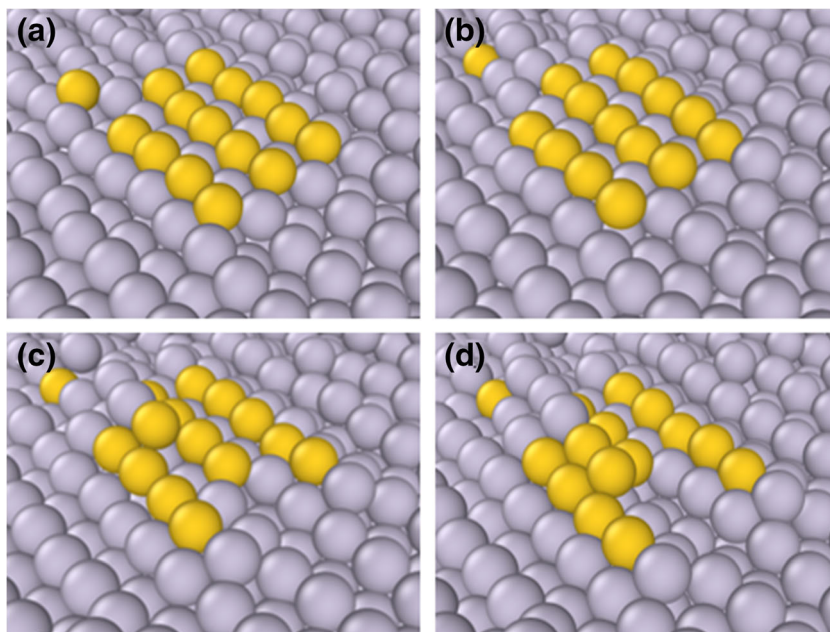
System	$n = 15$	$n = 18$	$n = 20$	$n = 21$	$n = 24$	$n = 30$	$n = 35$
$Au_n/Ag(110)$							
Adsorption Energy (eV)	58.07	69.26	76.91	81.26	92.85	115.58	134.91
Formation Energy (eV)	3.48	3.52	4.39	5.15	5.98	7.19	8.17

Fig. 3 Dynamic evolution of an island of form $Au_{15}/Ag(110)$ at 550 K. Snapshots were obtained after evolution during (a) $t = 68$ ps, (b) $t = 74$ ps, (c) $t = 135$ ps, and (d) $t = 183$ ps



550 K for the 35-atom cluster and 600 K for the 15- and 21-atom clusters. The temperature is a key factor in the surface diffusion activation and its attachment/detachment process of an adatom of island. In addition, each size of the island corresponds to a birth temperature of these processes. By way of example, the case of 15-sized island corresponds to 400 K and the case of 35-sized island corresponds to 650 K.

Figure 8 shows the response time of the 3D regime (3D growth mode) of the different island sizes as a function of temperature. We notice that the larger the size of the island,

the high temperature to initiate the 3D diffusion (C15 and C18 correspond to a temperature of 400 K, C21, C24, and C25 diffusion start at 450 K, while C30 and C35 correspond to 500 K). For all sizes, the time of the 3D mode shows a decrease upon increasing temperature and almost vanishes at 700 K.

Figure 9 shows the response time of the 3D regime versus the island size for different temperatures. It is shown that, at a temperature of 700 K the 3D mode is reached quickly, this response time increases as the temperature decreases, the same profile is found for 600 and 650 K with a shift in time. For 500

Fig. 4 Dynamic evolution of an island of form $Au_{21}/Ag(110)$ at 650 K: (a) exchange with an adatom from the substrate, (b) 2D to 3D transition and formation of homogeneous dimer, (c) formation of two heterogeneous trimers, and (d) formation of a 9-atom heterogeneous island. Snapshots were obtained after evolution during (a) $t = 8$ ps, (b) $t = 47$ ps, (c) $t = 187$ ps, and (d) $t = 276$ ps

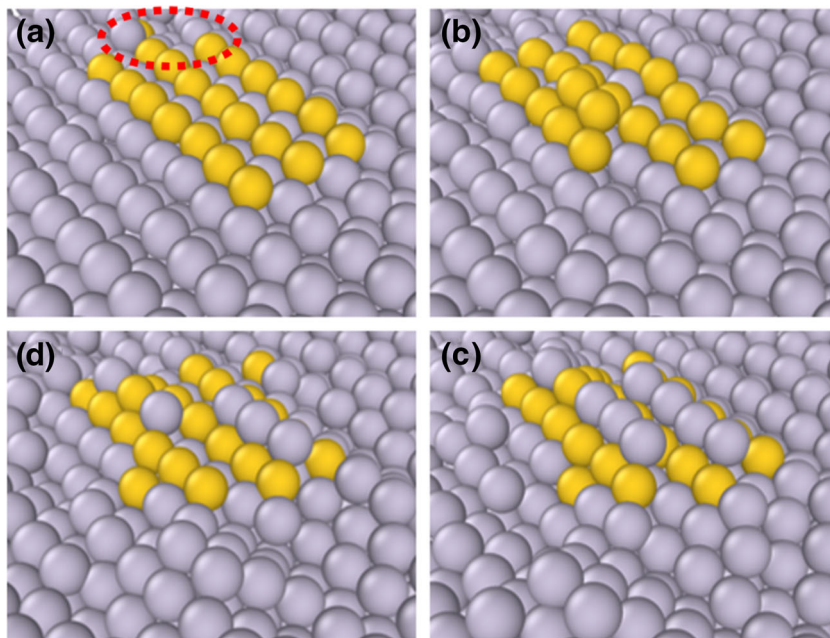
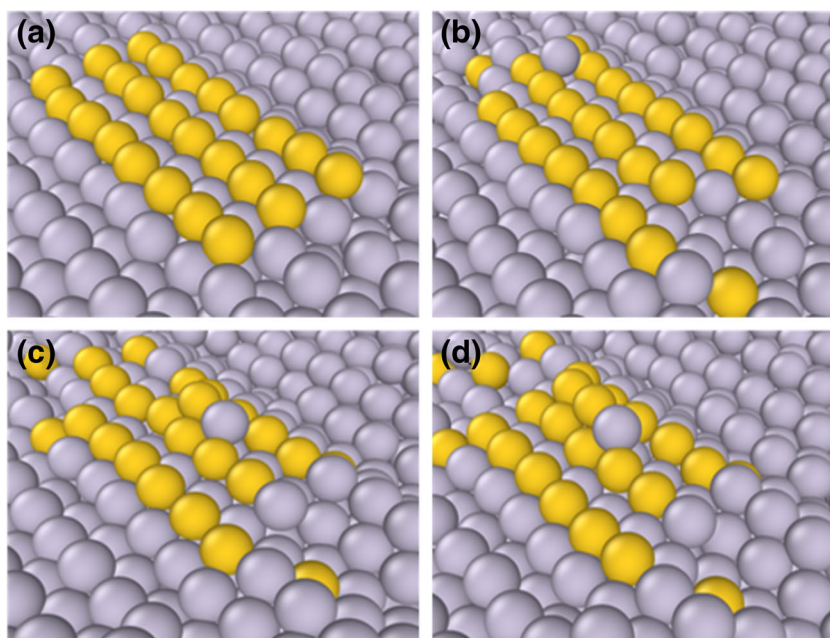


Fig. 5 Dynamic evolution of a shaped island $Au_{24}/Ag(110)$ at 600 K. **(a)** Islands of rectangle form, **(b)** 2D to 3D transition and formation of substrate adatom, **(c)** formation of a heterogeneous dimer, **(d)** formation of a heterogeneous trimer. Snapshots were obtained after evolution during **(a)** $t = 0$ ps, **(b)** $t = 74$ ps, **(c)** $t = 210$ ps, and **(d)** $t = 469$ ps



and 550 K, a 3D regime has appeared for small clusters between 15 and 20 adatoms while beyond this size the 3D regime is not reached (total disappearance). We can conclude then that the 3D regime does not appear at all for small clusters at low temperatures.

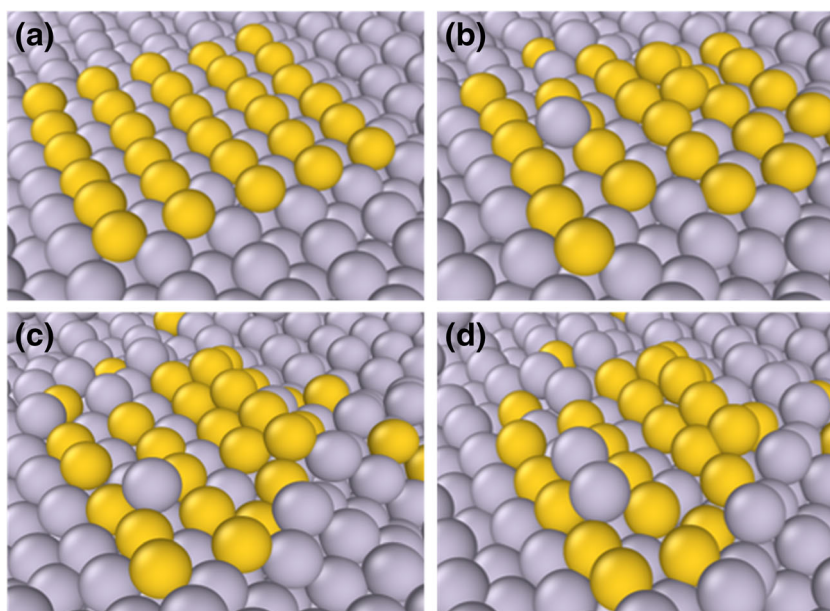
2D and 3D growth

Several techniques of epitaxial growth have been developed and differ in the operational mode as well as in the nature of the medium in contact with the substrate. In the present study, we define two growth rates:

The growth rate of a 3D island expressed by the ratio $\tau_{3D} = \frac{N_{3D}}{N_n} N_n \times 100$, with N_{3D} standing for the number of adatoms transformed to 3D and N_n is the total number of adatoms constituting the island (cluster size). The second parameter we can define is the 2D growth rate (attachment ratio) of an island that is defined by the ratio $\tau_{2D} = \frac{N_{2D}}{N_n} N_n \times 100$ where N_{2D} is the number of adatoms attached to the cluster at 2D.

Figure 10a plots the 3D growth rate versus temperature for different cluster sizes. We can distinguish between two regimes. Below 600 K, the rate τ_{3D} increases with the size of

Fig. 6 Dynamic evolution of a shaped island $Au_{30}/Ag(110)$ at 650 K. **(a)** square shaped islands, **(b)** 2D to 3D transition and formation of a homogeneous dimer and adatom on the substrate, **(c)** formation of a homogeneous tetramer and adatom on the substrate, **(d)** formation of a homogeneous tetramer and a substrate dimer. Snapshots were obtained after evolution during **(a)** $t = 0$ ps, **(b)** $t = 66$ ps, **(c)** $t = 184$ ps, and **(d)** $t = 274$ ps



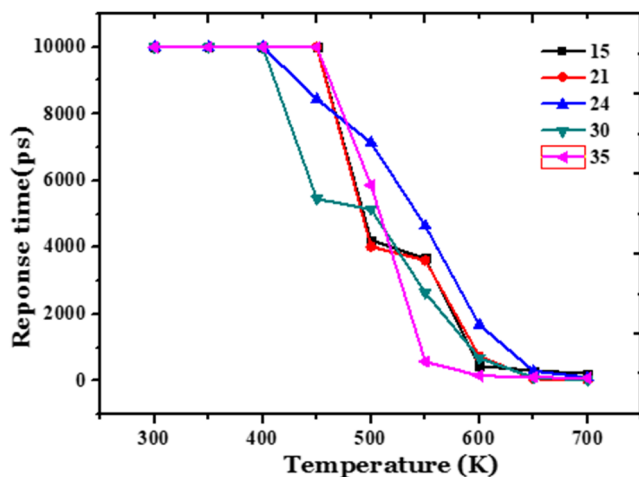


Fig. 7 Response time as a function of temperature for different island sizes

the island which promotes 3D growth. Furthermore, by comparing curves of C_{24} (with rectangular shape) with that of C_{30} (square shape), we may suggest that the shape of the island plays a significant role in the determination of the growth mode. Beyond 600 K, the C_{15} cluster shows the highest percentage of the 3D growth rate, with almost 50% of Au adatoms from the original cluster and 50% of adatoms segregated from the substrate. However, the largest island C_{30} shows the lowest τ_{3D} rate with 67% of Au adatoms coming from the cluster while 33% of Au adatoms came from the substrate. Consequently, we can suggest that the rectangular shape of the islands promotes 3D growth above 600 K by exchange mechanisms between Au and Ag adatoms.

Figure 10b shows the evolution of the attachment ratio τ_{2D} as a function of temperature for different cluster sizes. For C_{15} and C_{21} , the maximum of τ_{2D} is reached at 550 K; for C_{24} and C_{30} , the maximum attachment is obtained at 600 K while C_{35} shows a maximum at 650 K. Above this temperature, the

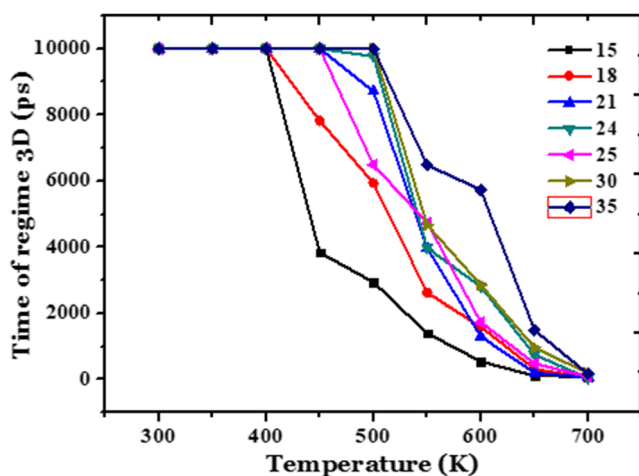


Fig. 8 The evolution of the response time needed for the 2D to 3D transition as a function of temperature for different cluster sizes

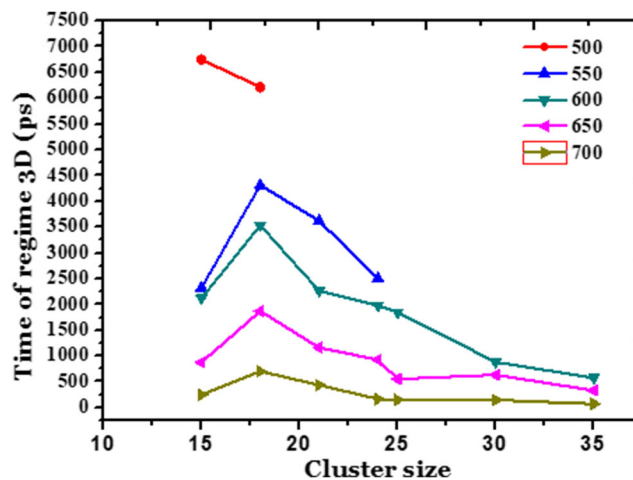


Fig. 9 The evolution of the response time needed for the 2D to 3D transition as a function of the cluster size at different temperatures

system disintegrates completely due to strong thermal activation. Consequently, larger clusters resist more than small ones.

Figure 11 presents the duration of stability of 2D islands as a function of temperature and cluster size. We can observe from Fig. 11a that, for low temperatures (450 and 500 K), the duration of stability increases by increasing cluster size, while it shows a slight decrease followed by an increase for higher temperatures. All curves have a tendency to saturate for larger clusters, which suggest that the larger the cluster the more stable it is. Figure 11b plots the stability time versus of temperature for different cluster sizes. We can deduce that C_{15} performs an almost linear increase versus temperature. The other clusters show a significant concavity, with a minimum that shifts to larger temperatures and loses its intensity for larger clusters.

Coalescence islands

In a second part of the present work, we focus on the coalescence of islands; we will follow the dynamic evolution of two islands during a period of 10 ns at different temperatures between 300 K and 700 K. A larger one which has been taken to be Au_{15} and a smaller one cluster Au_m with $(m = 0, 2, \dots, 9)$. These simulations are undertaken to understand the combination of two diffusion phenomena: the appearance of the 3D regime and the coalescence of islands according to the cluster size and temperature. We start each run by a configuration where a small cluster Au_m is brought next to a larger one Au_{15} . We then follow the dynamic behavior of the two clusters by inspecting snapshots showing their evolution during the considered time for different temperatures.

Figure 12 presents an example of the dynamic evolution of two islands Au_{15} ; $Au_2/Ag(110)$ at 550 K. We observed that C_{15} promotes the dissociation of the small Au_2 cluster to two adatoms, one gets attached to the mother cluster C_{15} (partial coalescence) (Fig. 12b) while the other adatom moves away

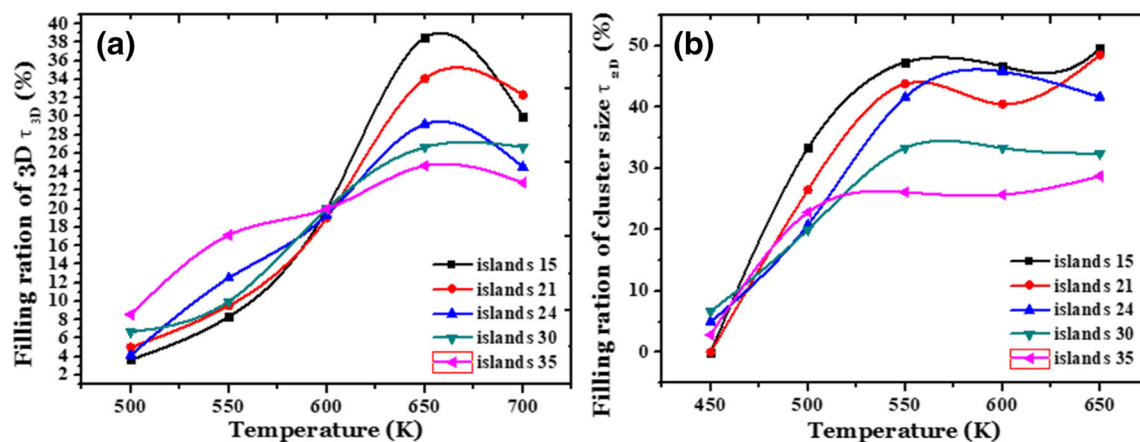


Fig. 10 The trend of the growth rate of different islands: (a) rate τ_{3D} of 3D island; (b) rate τ_{2D} of 2D island

from the big cluster by in-channel or exchange diffusion mechanisms. During this evolution, we noticed a transition from 2D to 3D by a homogeneous trimer (Fig. 12c), leading to the formation of a heterogeneous linear 3D stable trimer along the channel (Fig. 12d). Our study has shown that the exchange of Au island adatoms on Ag(110) surface occurs more easily near the edge of the ascending step parallel to the [110] direction than at the edge of descending step or on a terrace, which is in contradiction with the literature [34].

Figure 13 describes the dynamic evolution of two shape islands Au_{15} ; $Au_4/Ag(110)$ at 500 K. We noticed that the two islands are joined by attachment of a dimer (Fig. 13b) with a transformation of the tetramer from a square form to another form. Then, we obtain a homogeneous coalescence (Fig. 13c). During this evolution through exchange mechanisms, the system arrives at a 2D island (Fig. 13d).

Figure 14 illustrates an example of the dynamic evolution of two shape islands Au_{15} ; $Au_6/Ag(110)$ at 650 K (Fig. 14a). We observe that the small island C6 disintegrates by the exchange mechanism whereas the large island transforms to a 3D regime by an adatom making an over jump (Fig. 14b) by 0.18 eV in IC and 0.21 eV in CC (see Table 1). We suggest

that the bigger cluster will proceed by disintegrating the smaller one (up to hexamers) and then starts absorbing it. This process may be a precursor to the 3D transition by allowing adsorbed adatoms to make more exchange jumps (Fig. 14d).

Figure 15 corresponds to the dynamic evolution of two shape islands Au_{15} ; $Au_9/Ag(110)$ at 500 K (Fig. 15a). We see that the diffusion began by a detachment of an adatom from the larger cluster C15 followed by an attachment to the smaller cluster C9. This is accompanied by the occurrence of the 3D regime for C9 via an exchange jump (Fig. 15b). During this evolution, the larger cluster undergoes also a transition to the 3D regime by a similar jump (Fig. 15c). Other jump processes will contribute to the formation of a single bigger cluster containing 24 adatoms (Fig. 15d).

We have computed the response time of these islands by making the same type of calculation as what have been done for single clusters. The response time is the time necessary to trigger the diffusion of an island. Figure 16 presents the response time of the different mixtures of islands (complex islands with several attachments 2, 4, 6, and 9) together with that corresponding to the simple C15 for comparison. We notice that the C15 cluster resists more when it is isolated than

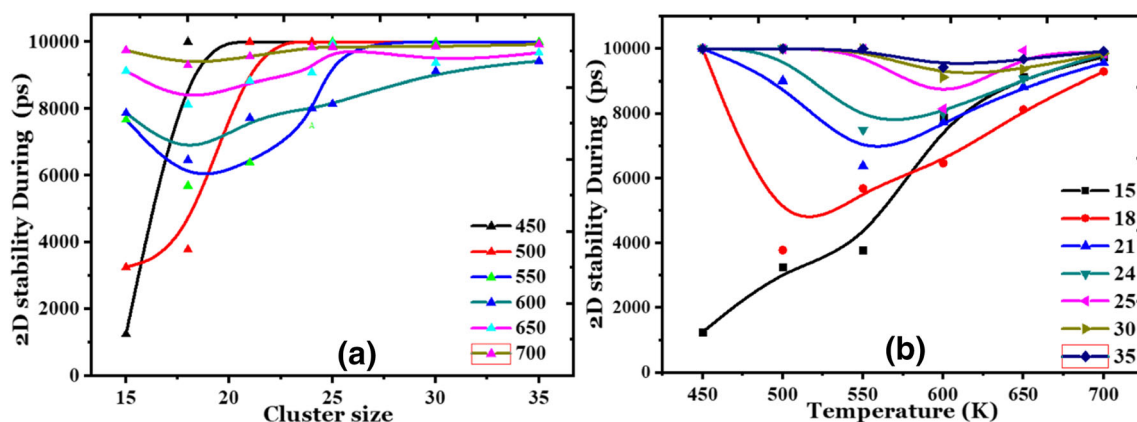
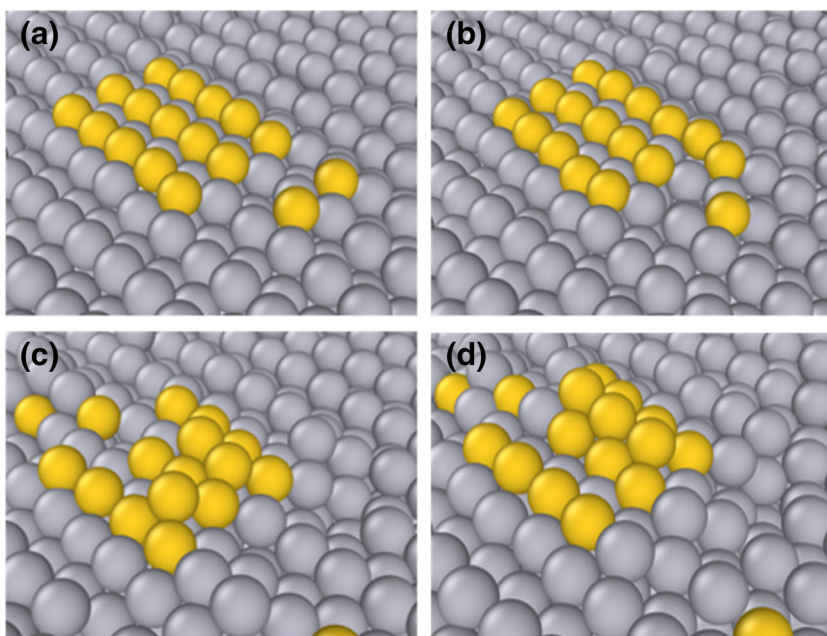


Fig. 11 The statistical study of 2D island stability as a function of (a) cluster size and (b) temperature

Fig. 12 Dynamic evolution of two shape islands Au_{15} ; $Au_2/Ag(110)$ at 550 K. Snapshots were obtained after evolution during (a) $t = 0$ ps, (b) $t = 136$ ps, (c) $t = 204$ ps, and (d) 291 ps



when it is attached to small clusters. From these results, we notice that the more the cluster size is larger the more the response time is longer, then, a progressive decrease is triggered before they reach their stability according to the evolution of the temperature. For $C15 + 9$, $C15 + 6$, and $C15 + 4$, the diffusion mechanisms are triggered at 450 K or the response time starts to decrease. However, in the case of $C15 + 2$, these mechanisms started at 350 K.

Figure 17a and b plot the response time of the 3D regime of the islands with attachments ranging from 2 to 9 adatoms. It is shown that the 3D regime resists by increasing the number of

attached adatom. We can see from Fig. 17b that it is easy to form the 3D mode at 700 K, confirmed by the short time needed to form this regime, which is about 500 ps. This response time increases by decreasing temperature for the different types of attachments mentioned above. This effect should be linked to the Schwoebel barrier that can be overcome easily at high temperatures.

The coalescence study led us to go deeper in our study and check a coalescence characteristic time as a function of the different parameters. Figure 18a and b plot this duration (which is defined as the elapsed time before the two clusters

Fig. 13 Dynamic evolution of two shape islands Au_{15} ; $Au_4/Ag(110)$ at 500 K. Snapshots were obtained after evolution during (a) $t = 0$ ps, (b) $t = 157$ ps, (c) $t = 369$ ps, and (d) $t = 821$ ps

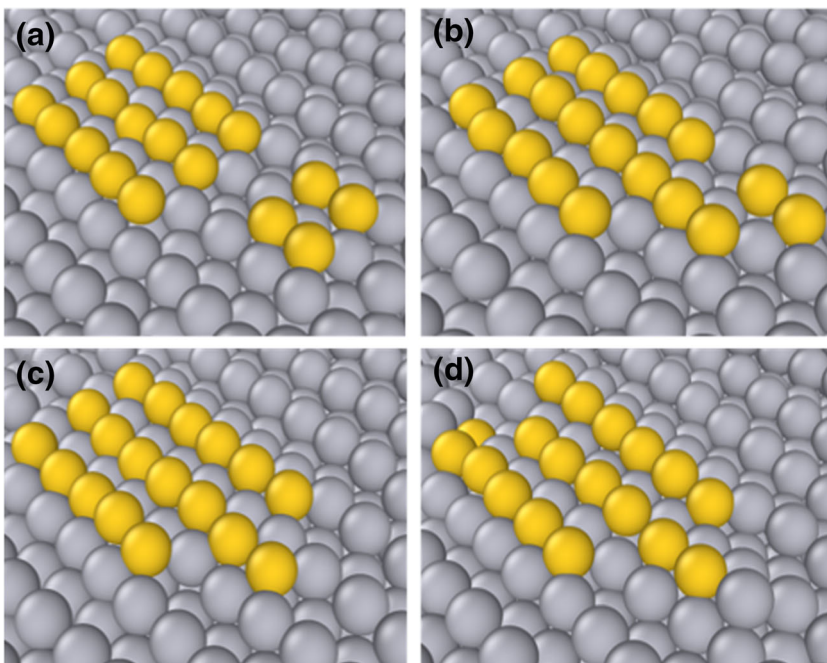
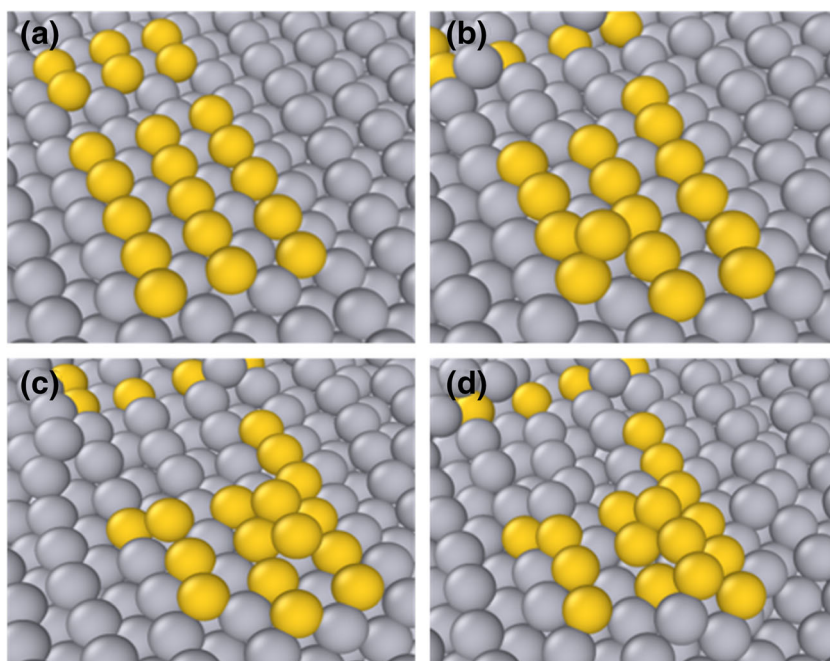


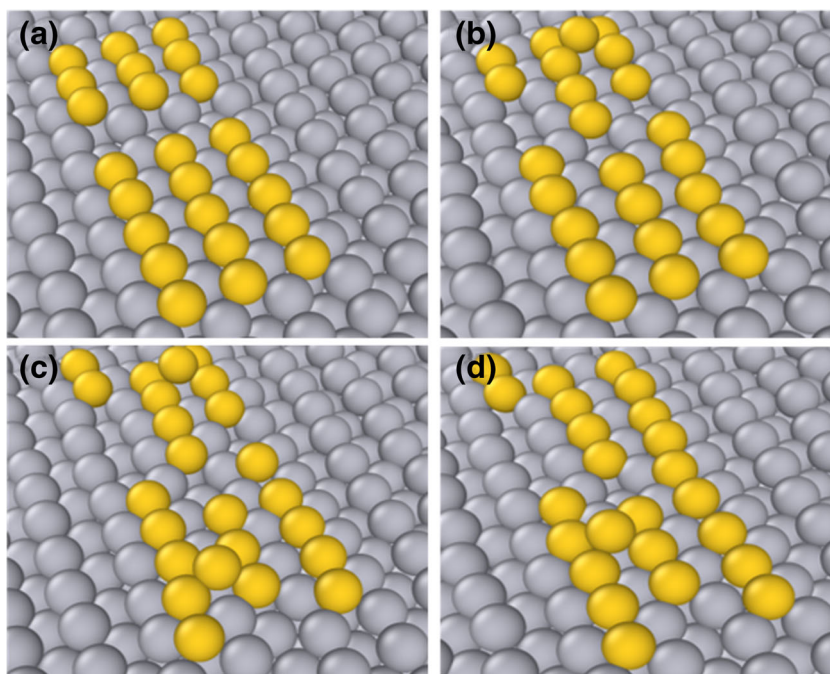
Fig. 14 Dynamic evolution of two shape islands Au_{15} ; $Au_6/Ag(110)$ to 650 K. Snapshots were taken at times (a) $t = 0$ ps, (b) $t = 108$ ps, (c) $t = 328$ ps, and (d) $t = 376$ ps



make contact) versus temperature and cluster size. We can deduce that the duration of coalescence depends on the size of the small cluster. Indeed, the coalescence lasts longer for larger absorbed clusters. This effect is accelerated by the increase of temperature which suggests that thermal vibration plays a major role in dissociation/re-association processes needed for coalescence phenomenon. The thermal activation accelerates the dissociation of small clusters into adatoms and

then favors their coalescence to large islands leading to the decrease of the coalescence time. Moreover, the thermal energy allows promoting the exchange/jump processes by overcoming the E_s barrier, which leads to the decrease of the response time. From another side, small clusters are easier to disintegrate into adatoms and migrate towards larger ones leading to premature coalescence, which explains why coalescence time increases with cluster size.

Fig. 15 Dynamic evolution of two shape islands Au_{15} ; $Au_9/Ag(110)$ to 500 K. Snapshots were obtained after evolution during (a) $t = 0$ ps, (b) $t = 595$ ps, (c) $t = 803$ ps, and (d) $t = 1739$ ps



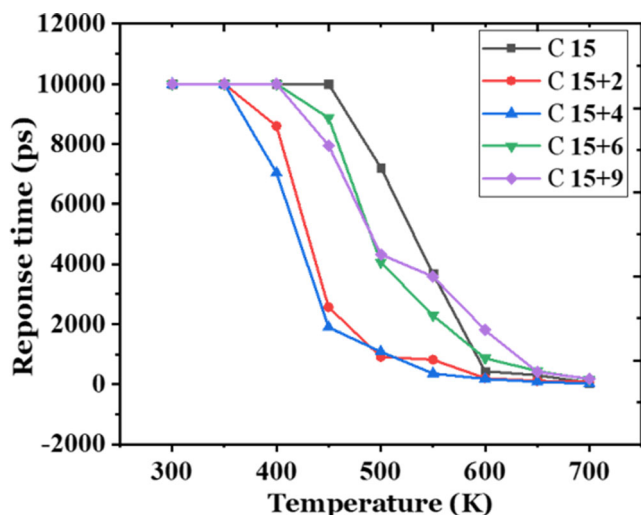


Fig. 16 Response time for different combinations of two islands as a function of temperature

Conclusion

The present study is based on the numerical simulation of the coalescence 2D-3D islands for Au on Ag(110) surface via the molecular dynamics method. The performed simulations supported island diffusion and thin film growth by both the 3D regime and cluster coalescence as the most dominant mechanism as opposed to the induced surface instability layer.

However, concerning different cluster sizes of the system Au_n/Ag(110) with 15 ≤ n ≤ 35, it can be concluded that the adsorption energy has higher values than the formation energy, which is explained by keeping track of the interaction of island adatoms with the substrate.

It was concluded that the effect of temperature plays a key role in obtaining the phenomenon of growth by the 2D to 3D transition which is a priority for large clusters, similarly, it was concluded that the phenomenon of growth by the coalescence

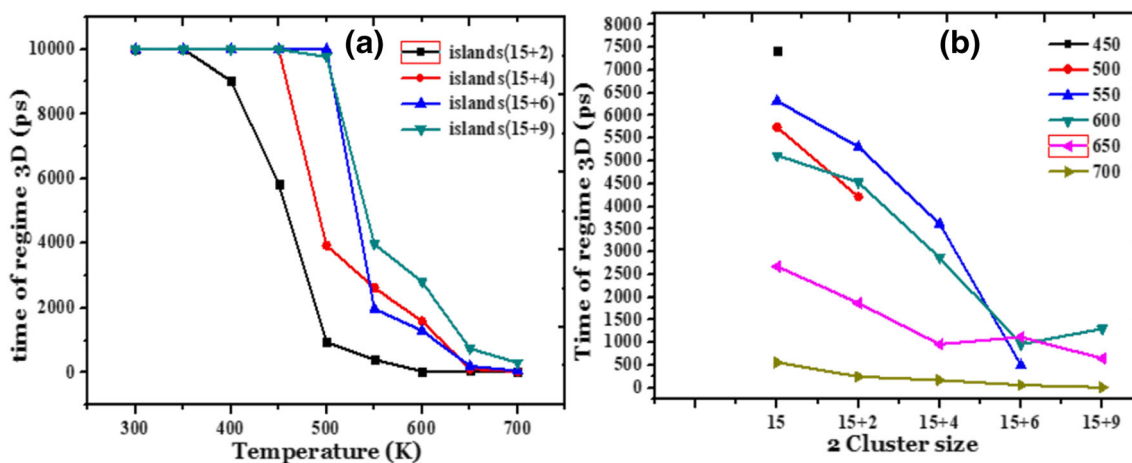


Fig. 17 Evolution of the response time of the 2D to 3D transition of two islands as a function of (a) temperature and (b) cluster size

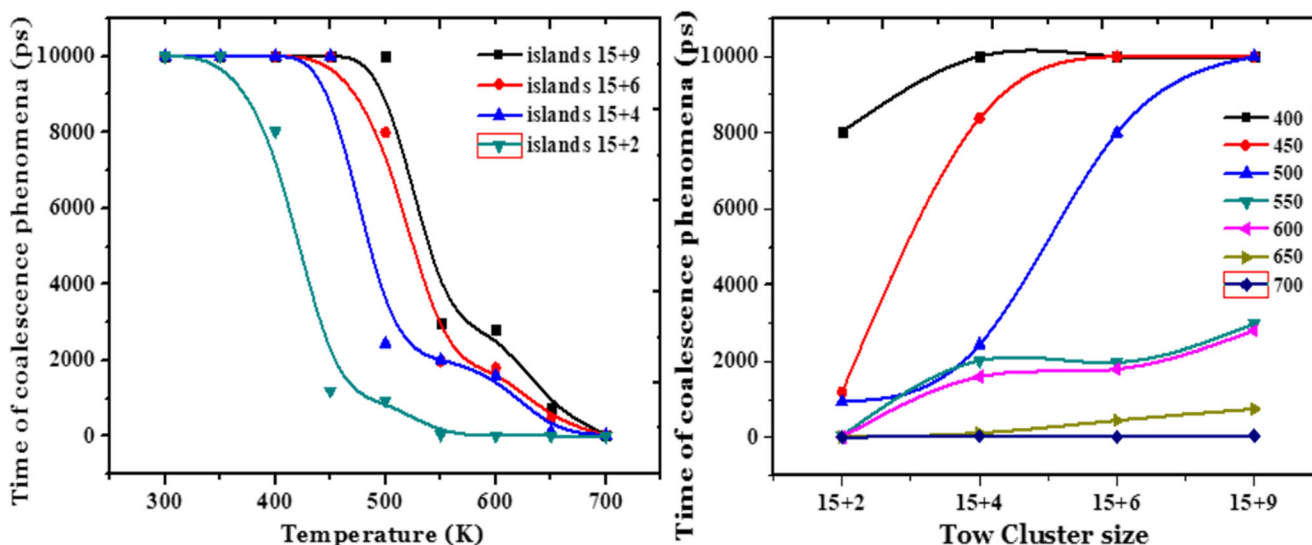


Fig. 18 The variation of the response time of the coalescence of two islands as a function of (a) temperature and (b) cluster size

of clusters has a priority for small islands that can be explained by the thermal activation of atoms. Also, the 3D mobility of gold adatoms is much higher than that of the 2D adatoms, which is in agreement with the results obtained by Michael et al. [35]. In addition to these results, we observed that the process of total disintegration of the clusters is only found for temperatures above 700 K for all systems Au_n ; $Au_m/Ag(110)$ ($n = 15, \dots, 35$; $m = 0, 2, \dots, 9$).

References

- S. Granneman, E. Petfalski, and D. Tollervey, "A cluster of ribosome synthesis factors regulate open," vol. 30, no. 19, pp. 4006–4019, 2011. <https://doi.org/10.1038/emboj.2011.256>
- Y. Xiang, X. Wu, D. Liu, X. Jiang, and W. Chu, "Formation of rectangularly shaped Pd/Au bimetallic nanorods: evidence for competing growth of the Pd shell between the { 110 } and { 100 } side facets of Au nanorods," pp. 2–6, 2006
- Kellogg GL (1994) Field ion microscope studies of single-atom surface diffusion and cluster nucleation on metal surfaces. *Surf. Sci. Rep.* 21(1–2):1–88. [https://doi.org/10.1016/0167-5729\(94\)90007-8](https://doi.org/10.1016/0167-5729(94)90007-8)
- Venables JA, Harding JH (2000) Nucleation and growth of supported metal clusters at defect sites on oxide and halide (001) surfaces. *J. Cryst. Growth* 211(1):27–33. [https://doi.org/10.1016/S0022-0248\(99\)00837-4](https://doi.org/10.1016/S0022-0248(99)00837-4)
- Henry CR (2000) Catalytic activity of supported nanometer-sized metal clusters. *Appl. Surf. Sci.* 164(1–4):252–259. [https://doi.org/10.1016/S0169-4332\(00\)00344-5](https://doi.org/10.1016/S0169-4332(00)00344-5)
- M. Shen et al., "Accelerated coarsening of Ag adatom islands on Ag (111) due to trace amounts of S: mass-transport mediated by Ag–S complexes vol. 094701, no. May 2012, 2009. <https://doi.org/10.1063/1.3078033>
- K. B. Gylfason et al., "Process considerations for layer-by-layer 3D patterning of silicon, using ion implantation, silicon deposition, and selective silicon etching" vol. 05, no. 2012, pp. 3–7, 2015. <https://doi.org/10.1116/1.4756947>
- H. J. Kim et al., "On the formation mechanism of epitaxial Ge islands on partially relaxed SiGe buffer layers," vol. 2257, no. 2004, 2015. <https://doi.org/10.1116/1.1775188>
- T. Kitajima, B. Liu, S. R. Leone, T. Kitajima, B. Liu, and S. R. Leone, "Two-dimensional periodic alignment of self-assembled Ge islands on patterned Si (001) surfaces" vol. 497, no. 001, pp. 2000–2003, 2003. <https://doi.org/10.1063/1.1434307>
- Hill H (2009) Fixing teacher professional development. *Phi Delta Kappan* 90:470–476. <https://doi.org/10.1177/0964663912467814>
- N. Motta, P. D. Szkutnik, M. Tomellini, and A. Sgarlata, "Role of patterning in islands nucleation on semiconductor surfaces," vol. 7, pp. 1046–1072, 2006. <https://doi.org/10.1016/j.crchy.2006.10.013>
- El Azrak H et al (2019) Investigation of fcc and hcp island nucleated during homoepitaxial growth of copper by molecular dynamics simulation. *Superlattice. Microst.* 127:118–122. <https://doi.org/10.1016/j.spmi.2017.12.056>
- Hassani A et al (2019) Superlattices and microstructures statistical investigations of the film-substrate interface during aluminum deposition on Ni (111) by molecular dynamics simulation. *Superlattice. Microst.* 127:80–85. <https://doi.org/10.1016/j.spmi.2018.03.008>
- Kherbouche EF, Annou R (2015) Behavior of Cu and Ni clusters landing at grazing incidence on Ni(001) and Cu(001) surfaces: molecular dynamics simulation. *Comput. Mater. Sci.* 110:353–358. <https://doi.org/10.1016/j.commatsci.2015.07.039>
- Nita F, Mastail C, Abadias G (2016) Three-dimensional kinetic Monte Carlo simulations of cubic transition metal nitride thin film growth. *Phys. Rev. B* 93:1–13. <https://doi.org/10.1103/PhysRevB.93.064107>
- Restrepo OA, Mousseau N (2017) Study of point defects diffusion in nickel using kinetic activation-relaxation technique *Acta Materialia. Acta Mater.* 144(2018):679–690. <https://doi.org/10.1016/j.actamat.2017.11.021>
- Marinica MC, Willaime F, Mousseau N (2011) Energy landscape of small clusters of self-interstitial dumbbells in iron. *Phys. Rev. B - Condens. Matter Mater. Phys.* 83:1–14. <https://doi.org/10.1103/PhysRevB.83.094119>
- Fu TY, Tsong TT (2001) Structure and diffusion mechanism of Ir and Rh tetramers on Ir (001) surfaces. *Surf. Sci.* 482–485:1249–1254. [https://doi.org/10.1016/S0039-6028\(01\)00906-2](https://doi.org/10.1016/S0039-6028(01)00906-2)
- Han Y, Stoldt CR, Thiel PA, Evans JW (2016) Ab initio thermodynamics and kinetics for coalescence of two-dimensional nanoislands and nanopits on metal (100) surfaces. *J. Phys. Chem. C* 120(38):21617–21630. <https://doi.org/10.1021/acs.jpcc.6b07328>
- Yang W, Zeman M, Ade H, Nemanich RJ (2003) Attractive migration and coalescence: a significant process in the coarsening of TiSi 2 islands on the Si (111) surface. *Phys. Rev. Lett.* 90(April):4–7. <https://doi.org/10.1103/PhysRevLett.90.136102>
- Van Siclen CD (1995) Single jump mechanisms for large cluster diffusion on metal surfaces. *Phys. Rev. Lett.* 75(8):1574–1577. <https://doi.org/10.1103/PhysRevLett.75.1574>
- Uberuaga BP, Marti E (2015) Mobility and coalescence of stacking fault tetrahedra in Cu. *Sci. Rep.* 5(V):1–5. <https://doi.org/10.1038/srep09084>
- Stoldt CR et al (2009) Smoluchowski ripening of Ag islands on Ag (100). *Chem. Phys.* (100):111, 5157. <https://doi.org/10.1063/1.479770>
- Dardouri M, Hassani A, Hasnaoui A, Arbaoui A, Boughaleb Y, Sbiaai K (2019) Kinetic Monte Carlo simulations of coverage effect on Ag and Au monolayers growth on Cu (110). *J. Cryst. Growth* 522(June):139–150. <https://doi.org/10.1016/j.jcrysgro.2019.06.024>
- Dardouri M, Sbiaai K, Hassani A, Hasnaoui A, Boughaleb Y (2019) Silver monolayer formation on Cu (110) by kinetic Monte Carlo. *Eur. Phys. J. Plus* 134:1–10. <https://doi.org/10.1140/epjp/i2019-12503-8>
- R. Gomer, "Diffusion of adsorbates on metal surfaces," *Reports on Progress in Physics*, vol. 53, no. October 1989, pp. 917–1002, 1990. <http://iopscience.iop.org/0034-4885/53/7/002>
- A. M. Shikin, D. V Vyalikh, Y. S. Dedkov, G. V Prudnikova, and V. K. Adamchuk, "Extended energy range of Ag quantum-well states in Ag (111)/Au (111)/W (110)," *Phys. Rev. B*, vol. 62, no. 4, pp. 2303–2306, 2000
- Fu TY, Hwang YJ, Tsong TT (2003) Structure and diffusion of Pd clusters on the W(110) surface. *Appl. Surf. Sci.* 219(1–2):143–148. [https://doi.org/10.1016/S0169-4332\(03\)00596-8](https://doi.org/10.1016/S0169-4332(03)00596-8)
- Wu Y et al (2012) Enhancement of Ag cluster mobility on Ag surfaces by chloridation. *Chem. Phys.* vol. 184705. <https://doi.org/10.1063/1.4759266>
- Sbiaai K et al (2012) Diffusion of Ag dimer on Cu (110) by dissociation-reassociation and concerted jump processes. *Int. Conf. Transparent Opt. Networks* 110:1–3. <https://doi.org/10.1109/ICTON.2012.6253824>
- Elkoraychy E, Sbiaai K, Mazroui M, Ferrando R, Boughaleb Y (2017) Heterodiffusion of Ag adatoms on imperfect Au (110) surfaces. *Chem. Phys. Lett.* 669:150–155. <https://doi.org/10.1016/j.cplett.2016.12.031>

32. Sbiaai K, Boughaleb Y, Mazroui M, Hajjaji A, Kara A (2013) Energy barriers for diffusion on heterogeneous stepped metal surfaces: Ag/Cu(110). *Thin Solid Films* 548:331–335. <https://doi.org/10.1016/j.tsf.2013.09.064>
33. Poteau R, Heully JL, Spiegelmann F (1997) Structure, stability, and vibrational properties of small silver cluster. *Zeitschrift fur Phys. D-Atoms Mol. Clust.* 40(1):479–482. <https://doi.org/10.1007/s004600050257>
34. Wang R, Fichthorn KA (1995) Kinetics of intermixing in Au/Ag(110) heteroepitaxy: a molecular-dynamics study. *Phys. Rev. B* 51(3):1957–1960. <https://doi.org/10.1103/PhysRevB.51.1957>
35. Haftel MI, Rosen M, Franklin T, Hettermann M (1994) Molecular dynamics observations of interdiffusion and Stranski-Krastanov growth in the early film deposition of Au on Ag(110). *Physical Review Lett* 72:12
36. Haftel MI, Rosen M (1995) Molecular-dynamics description of early film deposition of Au on Ag(110). *Phys. Rev.* 51(7):8. <https://doi.org/10.1103/PhysRevB.51.4426>
37. Yang Y et al (2013) Controlled growth of Ag/Au bimetallic nanorods through kinetics control. *Chem. Mater.* 25(1):34–41. <https://doi.org/10.1021/cm302928z>
38. Esplandi MJ, Schneeweiss MA, Kolb DM (1999) An in situ scanning tunneling microscopy study of Ag electrodeposition on Au (111). *Phys. Chem. Chem. Phys.* 1(111):4847–4854. <https://doi.org/10.1039/A906140A>
39. Fichthorn KA, Scheffler M (2000) Island nucleation in thin-film epitaxy: a first-principles investigation. *Phys. Rev. Lett.* 84(23):5371–5374. <https://doi.org/10.1103/PhysRevLett.84.5371>
40. Park C (1988) Growth of Ag, Au and Pd on Ru(0001) and CO chemisorption. *Surf. Sci* 203:395–411. [https://doi.org/10.1016/0039-6028\(88\)90090-8](https://doi.org/10.1016/0039-6028(88)90090-8)
41. Daw MS, Baskes MI (1984) Embedded-atom method: derivation and application to impurities, surfaces, and other defects in metals. *Phys. Rev. B* 29(12):6443–6453. <https://doi.org/10.1103/PhysRevB.29.6443>
42. Evans JW, Thiel PA, Bartelt MC (2006) Morphological evolution during epitaxial thin film growth: formation of 2D islands and 3D mounds. *Surf. Sci. Rep.* 61(1–2):1–128. <https://doi.org/10.1016/j.surfrep.2005.08.004>
43. M. Bon, N. Ahmad, R. Erni, and D. Passerone, “Reliability of two embedded atom models for the description of Ag @ Au nanoalloys,” *Phys. J Chem*, vol. 064105, no. April, 2019. <https://doi.org/10.1063/1.5107495>
44. Mottet C, Ferrando R, Hontinfinde F, Levi AC (1998) Simulation of the submonolayer homoepitaxial clusters growth on Ag(110). *Surf. Sci.* 417(1–4):220–237. <https://doi.org/10.1007/s100530050500>
45. Ndongmouo UT, Hontinfinde F (2004) Diffusion and growth on fcc(110) metal surfaces: a computational study. *Surf. Sci.* 571(1–3):89–101. <https://doi.org/10.1016/j.susc.2004.08.010>
46. Kyuno K, Ehrlich G (2000) Cluster diffusion and dissociation in the kinetics of layer growth: an atomic view. *Phys. Rev. Lett* 84:3. <https://doi.org/10.1103/PhysRevLett.84.2658>
47. Liu F, Hu W, Deng H, Luo W, Xiao S, Yang J (2009) Nuclear instruments and methods in physics research B energetics and self-diffusion behavior of Zr atomic clusters on a Zr (0001) surface. *Nucl. Inst. Methods Phys. Res. B* 267(18):3267–3270. <https://doi.org/10.1016/j.nimb.2009.06.055>

Publisher's note Springer Nature remains neutral with regard to jurisdictional claims in published maps and institutional affiliations.